

## PAPER



Cite this: *Soft Matter*, 2016, 12, 6812

Received 30th May 2016,  
Accepted 15th July 2016

DOI: 10.1039/c6sm01244b

www.rsc.org/softmatter

# Effect of temperature and electric field on 2D nematic colloidal crystals stabilised by vortex-like topological defects†

K. P. Zuhail and Surajit Dhara\*

We report experimental studies on 2D colloidal crystals of dimers stabilized by vortex-like defects in planar nematic and  $\pi/2$  twisted nematic cells. The dimers are prepared and self-assembled using a laser tweezer. We study the effect of temperature and electric field on the lattice parameters of the colloidal crystals. The lattice parameters vary with the temperature in the nematic phase and a discontinuous structural change is observed at the nematic to smectic-A phase transition. In the nematic phase, we observed a large change in the lattice parameters ( $\approx 30\%$ ) by applying an external electric field perpendicular to the plane of the 2D crystals. The idea and the active control of the lattice parameters could be useful for designing tunable colloidal crystals.

## I. Introduction

There has been growing interest in developing photonic crystals using self-assembled colloidal particles and tuning their optical properties by several means. Tuning has been attempted in various ways, such as by chemical methods,<sup>1,2</sup> field effects<sup>3,4</sup> and temperature variation.<sup>5,6</sup> In this context, self-assembled structures of colloidal particles in nematic liquid crystals appeared to have potential for making a tunable colloidal assembly.<sup>7,8</sup> The particles in nematic liquid crystals induce topological defects and particle-defect combinations are known as elastic dipoles or quadrupoles depending on the symmetry of the transverse components of the far-field director.<sup>9–15</sup> These dipoles have a natural tendency to self-assemble due to anisotropic elastic forces. The self-assembly of these colloids can be guided and controlled using laser tweezers to form several spectacular 1D, 2D and 3D structures, which are stabilized by singular defects.<sup>8,9,16–18</sup> An unusual defect structure in which a non-singular disclination loop with a vortex-like defect is formed when two collinear anti-parallel elastic dipoles are pushed.<sup>19–21</sup> This structure is named an escaped hyperbolic defect ring (EHDR) with a topological strength of  $-2$ . The loop encircles the line connecting two particles and forms dimers which are metastable in planar nematic (PN) cells (see in Fig. 1(b)). However, in twisted nematic (TN) cells, chirality escalates the spontaneous formation of non-singular colloidal dimers from anti-parallel dipoles.<sup>22</sup> In this paper, we for the first time show

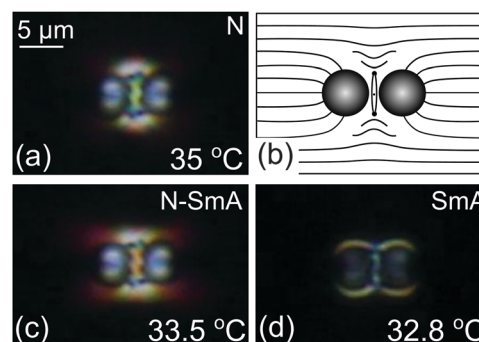


Fig. 1 Optical micrograph of a colloidal dimer with a vortex-like defect in the PN cell under crossed polarizers in the 8CB liquid crystal. (a) A dimer in the N phase, (b) schematic diagram of director orientation around the particles (adapted from ref. 21). (c) Transformation of defect at the N–SmA phase transition. (d) A dimer in the SmA phase. See ESI† (Video 1). Particle size 5.2  $\mu\text{m}$  and cell thickness 8.5  $\mu\text{m}$ .

the effect of temperature and an external electric field on the 2D crystals formed by colloidal dimers (stabilised by non-singular defects) used as building blocks. We show that the lattice parameters vary with temperature in the nematic phase followed by a structural change at the nematic to smectic-A phase transition. Above the Freedericksz threshold field we show a large decrease of the lattice constants with increasing electric field.

## II. Experimental

Experiments were performed in glass cells which were spin coated with polyimide (AL-1254) and cured at 100 °C for 1 h.

School of Physics, University of Hyderabad, Hyderabad, India.

E-mail: sdsp@uohyd.ernet.in

† Electronic supplementary information (ESI) available. See DOI: 10.1039/c6sm01244b

The PN cells were prepared by arranging the rubbing directions in an anti-parallel way. The TN cells were prepared by keeping the rubbing directions of the plates mutually perpendicular. In both the cells, a typical gap maintained is about 8  $\mu\text{m}$ . We used silica microspheres of (2R) 5.2  $\mu\text{m}$  diameter coated with DMOAP silane (octadecyldimethyl-3-trimethoxysilylpropyl-ammonium chloride) to induce strong homeotropic anchoring of liquid crystal molecules. The coated colloids are dispersed in 8CB (4'-*n*-octyl-4-cyano-biphenyl) and 5CB (4-cyano-4'-pentylbiphenyl) liquid crystals. 8CB and 5CB exhibit the following phase transitions: Cr. 21.5  $^{\circ}\text{C}$  SmA 33.5  $^{\circ}\text{C}$  N 40.5  $^{\circ}\text{C}$  I and Cr. 22  $^{\circ}\text{C}$  N 35  $^{\circ}\text{C}$  I, respectively. The electric field is applied using a function generator (Tektronix-AFG3102) and a voltage amplifier (TEGAM-2350). A laser tweezer was built around an inverted microscope (Nikon eclipse Ti-U) using a CW diode pumped solid state laser operating at 1064 nm (Aresis: Tweez 250si). A computer interfaced acousto-optic deflector was used for the trap movement. The temperature of the sample was controlled by a home-built heater and a proportional-integral-derivative (PID) controller with an accuracy of  $\pm 0.1$   $^{\circ}\text{C}$ . The trajectories of the particles were video recorded using a CCD camera (IDS-UI) at 20 frames per second. The center-to-center distance between the particles was measured from the video analysis and particle tracking software with a resolution of  $\pm 10$  nm.

### III. Results and discussion

To study the effect of temperature and also the N–SmA phase transition on the 2D colloidal crystals we selected 8CB liquid crystal. In the nematic phase, in PN cells, two collinear and parallel elastic dipoles are attracted and antiparallel dipoles are repelled. However, if the anti-parallel collinear dipoles are strongly pushed together using the optical tweezer it forms a dimer, which is connected by an escaped non-singular defect. This defect is also known as the “bubblegum defect”.<sup>19–21</sup> Fig. 1(a) shows an image of such a dimer in the nematic phase of 8CB. The local frustration in the director field between the colloids is clearly observed in the POM (polarizing optical microscopy) images (Fig. 1(a)). The director field around the bubblegum is known to be axially symmetric, minimally distorted and continuous (Fig. 1(b)). Fig. 1(c) and (d) show the transformation of the bubblegum defect when the temperature changes from the N to the SmA phase. The director distortion between the colloids and in their surroundings expands as the SmA transition is approached (Fig. 1(c)). In the SmA phase, the distortion shrinks to narrow regions (the bright incomplete rings in Fig. 1(d)) around the particles except the left and right hand sides of the dimer. The video of this transition and the temperature variation of the center to center separation between the particles across the phase transition are given in the ESI.<sup>†</sup><sup>23</sup> It shows that the equilibrium separation is linearly proportional to the elastic anisotropy,  $\Delta K$  ( $=K_{33} - K_{11}$ , where  $K_{33}$  and  $K_{11}$  are the bend and splay elastic constants). Recently we have shown the transformation of dipoles,<sup>16</sup> quadrupoles<sup>17</sup> and boojum defects<sup>8</sup> across the N–SmA phase transition. The observed rings around the particles

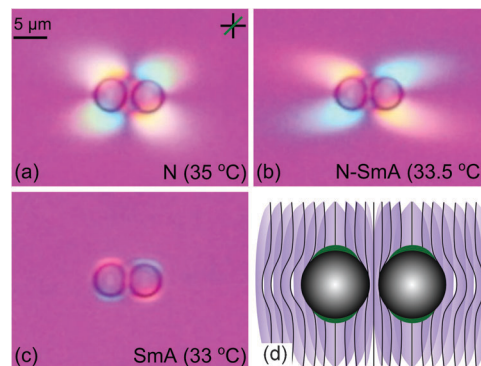
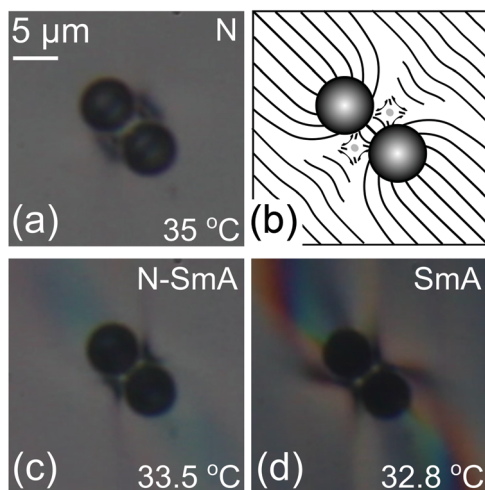


Fig. 2 Optical micrograph of a colloidal dimer with a vortex-like defect in the PN cell with the  $\lambda$ -plate (green line denotes the slow axis) between the analyzer and the sample in the CCN-47 liquid crystal. (a) A dimer in the N phase, (b) at the N–SmA phase transition, (c) in the SmA phase, (d) schematic diagram (based on (c)) of the SmA layers around the particles. In the SmA phase, the boundary condition is incompatible with the layer structure above and below the particles (green regions). Particle size 5.2  $\mu\text{m}$  and cell thickness 8.5  $\mu\text{m}$ .

in the SmA phase in Fig. 1(d) are somewhat similar to the one that was observed in the case of a quadrupolar defect in the SmA phase.<sup>17</sup> At the transition the particles appear to be touching each other however careful measurement shows that there is about a 0.6  $\mu\text{m}$  gap between them (see ESI,<sup>†</sup> Fig. S1) and the gap increases with decreasing temperature in the SmA phase.

To get more insight into the defect and SmA layer orientation around the particles we have chosen the CCN-47 (4'-butyl-4-heptyl-bicyclohexyl-4-carbonitrile) liquid crystal. It exhibits the following phase transition: Cr. 25.6  $^{\circ}\text{C}$  SmA 28.4  $^{\circ}\text{C}$  N 58.2  $^{\circ}\text{C}$  I. It has very low birefringence ( $\Delta n \simeq 0.03$ ), hence it is useful for understanding SmA layer orientation around the particles.<sup>24–26</sup> Fig. 2 shows the image of a dimer across the N–SmA phase transition in a PN cell with a  $\lambda$ -plate (red-plate). Here the red color corresponds to a horizontal orientation of the long axes of the molecules, whereas bluish and yellowish colors (Fig. 2(a) and (b)) correspond to clockwise and anti-clockwise rotation of the director from the rubbing direction, respectively. Interestingly in the SmA phase (Fig. 2(c)) we observe rings with opposite color above and below each particle. In addition, above the particles the rings (left and right) have opposite color. These rings are highly confined region of SmA layers that prevents extensive layer distortion due to incompatible boundary conditions of the particles. It suggests that the non-singular defect disappears at the transition and the SmA layers are nearly parallel in the narrow region observed between the particles. Based on this we propose a simple model of SmA layer orientation around the dimer in Fig. 2(d).

In TN cells, the director twists by 90 $^{\circ}$  from the bottom to the top substrate, and the elastic dipoles are spontaneously attracted and finally their joining line is oriented at 45 $^{\circ}$  with respect to both the rubbing directions (Fig. 3(a)). A vortex-like defect is formed between two particles (Fig. 3(b)) although the director distortion is very different from that of the PN cell (see Fig. 1(b)). The defect ring has four fold rotational symmetry enabling four distinct directions for the assembly mechanism.<sup>21</sup>



**Fig. 3** Optical micrograph of a colloidal dimer with a vortex-like defect in the TN cell under crossed polarizers in the 8CB liquid crystal. (a) A dimer in the N phase. (b) Schematic diagram of director orientation around the particles (adapted from ref. 21). (c) Transformation of defect at the N–SmA phase transition. (d) A dimer in the SmA phase. See ESI† (Video 2). Particle size 5.2  $\mu\text{m}$  and cell thickness 8.5  $\mu\text{m}$ .

Fig. 3(c) and (d) show the transformation of the defect of a colloidal dimer across the N–SmA phase transition. Near the transition point the director distortion increases and finally in the SmA phase, a very complex layer distortion is observed (Fig. 3(d)). A video of this transition and the temperature variation of the center to center separation between the particles across the phase transition are given in the ESI.†<sup>23</sup> The effect of temperature change on the colloidal dimers in both PN and TN cells is similar. In both cases the equilibrium separation between the particles in a dimer is governed by elastic anisotropy. The discontinuous change of the equilibrium separation at the N–SmA transition is due to the disappearance of non-singular defects and this is also an indicator of discontinuity in the elastic constants. However the temperature dependence of the equilibrium separation ( $D$ ) in the SmA phase is different. In particular, in the PN cell,  $D$  shows a critical behavior whereas in the TN cell it is independent of temperature (see ESI†).

Using two types of dimers as building blocks, we prepared two differently assembled 2D colloidal crystals using the optical tweezers and studied the effect of temperature and electric field on the lattice parameters. First we discuss the 2D crystals of dimers made of antiparallel elastic dipoles in the PN cell. Fig. 4(a) shows a 2D crystal made of 36 dimers (72 particles). The equilibrium lattice parameters at 36  $^{\circ}\text{C}$  are:  $a = b = 10.2 \pm 0.05 \mu\text{m}$ ,  $D = 6.4 \pm 0.05 \mu\text{m}$  and  $\phi = 45 \pm 1^{\circ}$  in the nematic phase. The temperature of the sample is decreased (at 0.3  $^{\circ}\text{C min}^{-1}$ ) across the N to SmA phase transition and the lattice parameters are measured as a function of temperature (see ESI,† Video 3). The temperature variation of the lattice parameters  $a$ ,  $b$  and  $D$  are shown in Fig. 4(e). All the lattice parameters tend to increase slightly followed by a discontinuous jump at the N–SmA transition. The SmA 2D crystal is more compact than that of the nematic phase. The corresponding polarizing optical microscopy

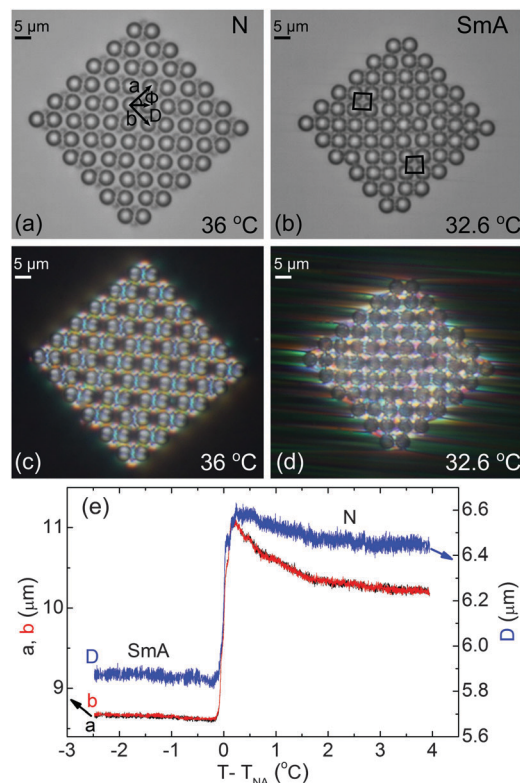


**Fig. 4** Optical photomicrograph of a 2D colloidal crystal in the N phase (36  $^{\circ}\text{C}$ ) and in the SmA phase (32.6  $^{\circ}\text{C}$ ) of the 8CB liquid crystal in the PN cell made of antiparallel dipoles (a and b) without polarizers; (c and d) between crossed polarizers. (e) Temperature variation of the lattice parameters  $a$ ,  $b$  and  $D$  across the N–SmA transition. See ESI† (Video 3). Cell thickness 8.5  $\mu\text{m}$ .

images are also shown in Fig. 4(c) and (d). In the N phase, between two neighboring dimers there are periodic voids of uniform nematic region. In the SmA phase strong distortion of layers is observed and the director distortion surrounding the particles is extended up to a few micrometer distance. In the SmA phase (32.6  $^{\circ}\text{C}$ ) the lattice parameters are:  $a = b = 8.6 \pm 0.05 \mu\text{m}$ ,  $D = 5.9 \pm 0.05 \mu\text{m}$  and  $\phi = 42 \pm 1^{\circ}$ . Thus lattice constants in the SmA phase ( $a$  and  $b$ ) are lower by  $\sim 16\%$  and  $D$  is lower by  $\sim 7\%$  with respect to the nematic phase. Consequently the area of the 2D crystal decreases from 2650  $\mu\text{m}^2$  (nematic phase) to 2100  $\mu\text{m}^2$  (SmA phase), which is about 21% reduction.

Fig. 5(a) shows a 2D crystal made of dimers in the TN cell of the 8CB liquid crystal. The temperature of the sample is decreased (0.3  $^{\circ}\text{C min}^{-1}$ ) across the N to SmA phase transition and the lattice parameters are measured as a function of temperature (see ESI,† Video 4). Fig. 5(b) shows a more compact structure in the SmA phase than in the nematic phase. The corresponding polarizing optical microscopy images are shown in Fig. 5(c) and (d). The structure of the SmA 2D crystal in the TN cell is very different from that of the PN cell. In particular, two neighboring dimers are connected by a cross-type texture in TN cells (Fig. 5(d)). The variation of the lattice parameters  $a$ ,  $b$  and  $D$  as a function of temperature is shown in Fig. 5(e). In the N phase at 36  $^{\circ}\text{C}$ , the equilibrium lattice parameters are:

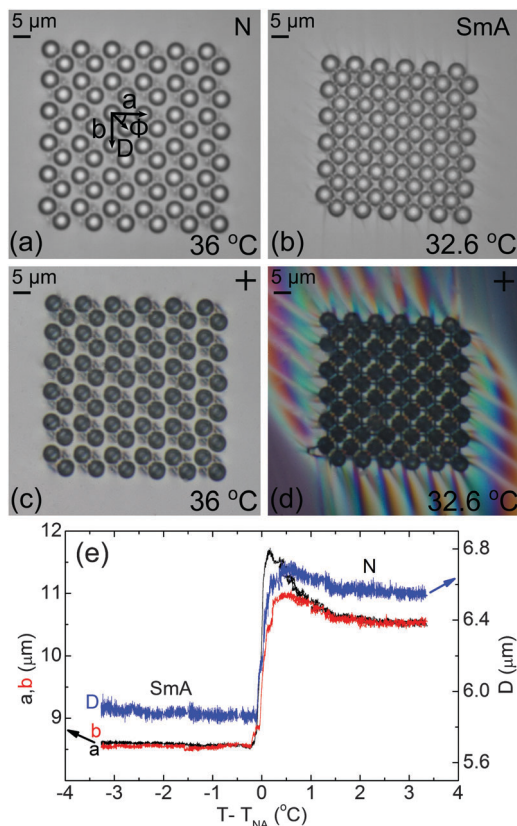


Fig. 5 Optical photomicrograph of a 2D colloidal crystal in the N phase (36 °C) and in the SmA phase (32.6 °C) in the TN cell of the 8CB liquid crystal (a and b) without polarizers and (c and d) between crossed polarizers. (e) Temperature variation of the lattice parameters;  $a$ ,  $b$  and  $D$  across the N–SmA transition. See ESI† (Video 4). Cell thickness 8.5  $\mu\text{m}$ .

$a = b = 10.5 \pm 0.05 \mu\text{m}$ ,  $D = 6.5 \pm 0.05 \mu\text{m}$  and  $\phi = 45 \pm 1^{\circ}$  (Fig. 5(a)). In the SmA phase at 32.6 °C, the lattice parameters are reduced, for example, at the highest field:  $a = b = 8.5 \pm 0.05 \mu\text{m}$ ,  $D = 5.9 \pm 0.05 \mu\text{m}$  and  $\phi = 45 \pm 1^{\circ}$  (Fig. 5(b)). The SmA lattice constants,  $a$  and  $b$ , are lower by 19% and  $D$  is lower by 9% with respect to the nematic phase. The area of the colloidal crystal decreases from 3050  $\mu\text{m}^2$  (nematic phase) to 2150  $\mu\text{m}^2$  (SmA phase), which is about 29% reduction. The process of controlling the lattice parameters by temperature in the TN cell is completely reversible while in the case of the PN cell it is mostly irreversible.

Finally we discuss the effect of an electric field on the 2D crystals in both PN and TN cells in the 5CB liquid crystal at room temperature (see ESI†, Video 5). The equilibrium lattice parameters are measured as a function of the applied electric field. Fig. 6(a) shows an image of a 2D crystal in the PN cell at zero field and Fig. 6(b) shows the image taken at the highest field (1  $\text{V} \mu\text{m}^{-1}$ ) above which the lattice constants do not decrease. It is observed that the lattice constants tend to increase slightly up to the Fredericksz threshold field ( $\approx 0.04 \text{V} \mu\text{m}^{-1}$ ) and then decrease with increasing field (Fig. 6(c)). For example, at room temperature and zero field,  $a = b = 10.2 \pm 0.05 \mu\text{m}$  and  $D = 6.4 \mu\text{m}$  and it decreases to  $a = b = 7.3 \pm 0.05 \mu\text{m}$  and  $D = 5.7 \mu\text{m}$  at a field of 1  $\text{V} \mu\text{m}^{-1}$ .

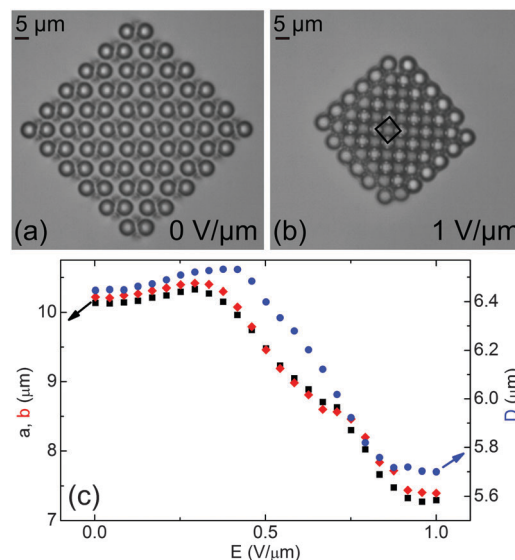


Fig. 6 Optical photomicrograph of a 2D colloidal crystal in a PN cell of the 5CB liquid crystal at (a) zero field and at (b) 1  $\text{V} \mu\text{m}^{-1}$ . (c) Variation of the lattice parameters  $a$ ,  $b$  and  $D$  as a function of the applied electric field at a frequency of 1 kHz. See ESI† (Video 5). Cell thickness 8.5  $\mu\text{m}$ .

Thus, the lattice parameters  $a$  and  $b$  decrease by  $\sim 28\%$  and  $D$  decreases by  $\sim 11\%$  at the highest field. The area of the 2D crystal decreases from 3000  $\mu\text{m}^2$  (0  $\text{V} \mu\text{m}^{-1}$ ) to 1600  $\mu\text{m}^2$  which is about 46% smaller compared to the area at zero field.

Fig. 7 shows the effect of electric field on the 2D crystal in the TN cell in the 5CB liquid crystal (see ESI†, Video 6). The lattice constants are measured as a function of field in the same way as we discussed. It is observed that the lattice parameters tend to increase slightly up to the threshold field ( $\approx 0.6 \text{V} \mu\text{m}^{-1}$ )

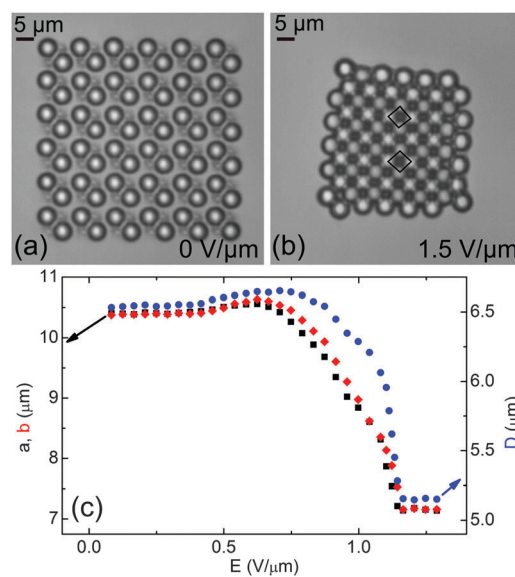


Fig. 7 Optical photomicrograph of a 2D colloidal crystal in a TN cell of the 5CB liquid crystal under the field, (a) 0  $\text{V} \mu\text{m}^{-1}$  and (b) 1.5  $\text{V} \mu\text{m}^{-1}$ . (c) Variation of the lattice parameters  $a$ ,  $b$  and  $D$  as a function of the applied electric field at a frequency of 1 kHz. See ESI† (Video 6). Cell thickness 8.5  $\mu\text{m}$ .

and then continuously decrease with increasing electric field up to  $1.15 \text{ V } \mu\text{m}^{-1}$  (Fig. 7(c)). For example, the lattice constants at zero field and at room temperature are:  $a = b = 10.4 \pm 0.05 \text{ } \mu\text{m}$  and  $D = 6.5 \text{ } \mu\text{m}$ . At the highest field ( $1.5 \text{ V } \mu\text{m}^{-1}$ ), it decreases to  $a = b = 7.1 \pm 0.05 \text{ } \mu\text{m}$  and  $D = 5.71 \text{ } \mu\text{m}$ . Thus  $a$  and  $b$  show  $\sim 31\%$  and  $D$  shows  $\sim 21\%$  decrease at the highest field. The area of the 2D crystal also decreases from  $3000 \text{ } \mu\text{m}^2$  ( $0 \text{ V } \mu\text{m}^{-1}$ ) to  $1650 \text{ } \mu\text{m}^2$  ( $1.5 \text{ V } \mu\text{m}^{-1}$ ) which is about a 45% reduction compared to the crystal area measured at zero field. The process of controlling the lattice parameters by field in both the cells is completely reversible.

The temperature variation of the lattice parameters is mainly due to the variation of elastic constants. In particular, the increase of the lattice parameters with decreasing temperature is due to the rapid increase of the bend elastic constant compared to the splay elastic constant. The discontinuity of the elastic constants at the N-SmA transition is marked by a discontinuous change of the lattice parameters. The effect of an electric field on the colloidal crystals can be expected due to the combined effect of nematic elasticity, the response of the nematic to the external electric field and the field-induced dipole-dipole interaction (electric) between the colloids.<sup>7</sup> In the low field range of the present experiment, the latter effect may not have a significant contribution. The director is highly nonuniform throughout the 2D crystals and hence there is no sharp threshold field of elastic deformation; consequently there are small deformations inside the 2D crystals which try to push the particles apart. On the other hand the nematic deformation outside the 2D crystal region, above the Freedericksz threshold field, exerts pressure on the crystal and its volume shrinks.

## IV. Conclusion

In conclusion, we have shown a structural response of 2D colloidal crystals (stabilized by bubblegum defects in planar and twisted nematic cells) to temperature variation and an external electric field. In the nematic phase the equilibrium separation between the particles weakly depends on temperature followed by a discontinuous structural change at the N-SmA phase transition. In the SmA phase the surrounding liquid crystal compresses the 2D crystals and the area of the crystals decreases significantly in both planar and twisted cells. The electric field response was studied only in the nematic phase as the 2D crystals in the SmA phase do not respond to the applied field. Above the Freedericksz threshold field, the surrounding medium compresses the 2D crystals. The inter-dimer spacing decreases by about 30% due to the applied electric field and consequently the areas of the 2D crystals decrease significantly. Based on this concept large electrically and thermally tunable colloidal crystals could be designed which may be useful for tunable photonic crystals.

## Acknowledgements

S. D. acknowledge support from DST-PURSE and a Swarnajayanti fellowship (DST/SJF/PSA-02/2014-2015). K. P. Z. acknowledges UGC for a fellowship.

## References

- 1 J. H. Holtz and S. A. Asher, *Nature*, 1997, **389**, 829.
- 2 Y. Kang, J. J. Walish, T. Gorishny and E. Thomas, *Nat. Mater.*, 2007, **6**, 957.
- 3 J. Xia, Y. Ying and S. H. Foulger, *Adv. Mater.*, 2005, **17**, 2463.
- 4 M. Aschwanden and A. Stemmer, *Opt. Lett.*, 2006, **31**, 2610.
- 5 J. M. Weissman, H. B. Sunkara, A. S. Tse and S. A. Asher, *Science*, 1996, **274**, 959.
- 6 B. Wild, R. Ferrini, R. Houdre, M. Mulot, S. Anand and C. J. M. Smith, *Appl. Phys. Lett.*, 2004, **84**, 846.
- 7 M. Humar, M. Škarabot, M. Ravnik, S. Žumer, I. Poberaj, D. Babić and I. Musević, *Eur. Phys. J. E: Soft Matter Biol. Phys.*, 2008, **27**, 73.
- 8 K. P. Zuhail and S. Dhara, *Appl. Phys. Lett.*, 2015, **106**, 211901.
- 9 P. Poulin, H. Stark, T. C. Lubensky and D. A. Weitz, *Science*, 1997, **275**, 1770.
- 10 I. Mušević, M. Škarabot, U. Tkalec, M. Ravnik and S. Žumer, *Science*, 2006, **313**, 954.
- 11 T. C. Lubensky, D. Pettey, N. Currier and H. Stark, *Phys. Rev. E: Stat. Phys., Plasmas, Fluids, Relat. Interdiscip. Top.*, 1998, **57**, 610.
- 12 H. Stark, *Phys. Rep.*, 2001, **351**, 387.
- 13 Y. Gu and N. L. Abbott, *Phys. Rev. Lett.*, 2000, **85**, 4719.
- 14 R. W. Ruhwandl and E. M. Terentjev, *Phys. Rev. E: Stat. Phys., Plasmas, Fluids, Relat. Interdiscip. Top.*, 1997, **55**, 2958.
- 15 H. Stark, *Phys. Rev. E: Stat., Nonlinear, Soft Matter Phys.*, 2002, **66**, 032701.
- 16 K. P. Zuhail, P. Sathyanarayana, D. Seč, M. Škarabot, I. Mušević and S. Dhara, *Phys. Rev. E: Stat., Nonlinear, Soft Matter Phys.*, 2015, **91**, 030501(R).
- 17 K. P. Zuhail, S. Čopar, I. Mušević and S. Dhara, *Phys. Rev. E: Stat., Nonlinear, Soft Matter Phys.*, 2015, **92**, 052501.
- 18 A. Nych, U. Ognysta, M. Škarabot, M. Ravnik, S. Žumer and I. Mušević, *Nat. Commun.*, 2013, **4**, 1489.
- 19 P. Poulin, V. Cabuil and D. A. Weitz, *Phys. Rev. Lett.*, 1997, **79**, 4862.
- 20 J. Fukuda and H. Yokoyama, *Phys. Rev. Lett.*, 2005, **94**, 148301.
- 21 U. Tkalec and I. Mušević, *Soft Matter*, 2013, **9**, 8140.
- 22 U. Tkalec, M. Ravnik, S. Žumer and I. Mušević, *Phys. Rev. Lett.*, 2009, **103**, 127801.
- 23 See ESI† for temperature variation of interparticle separation in dimers in PN and TN cells across the N-SmA phase transition in the 8CB liquid crystal. Several video clips showing transformation of defects across the phase transition and the effect of the electric field on the lattice parameters of 2D colloidal crystals in the 5CB liquid crystal.
- 24 S. Dhara and N. V. Madhusudana, *Europhys. Lett.*, 2004, **67**, 411.
- 25 S. Dhara and N. V. Madhusudana, *Phase Transitions*, 2008, **81**, 561.
- 26 T. A. Kumar, P. Sathyanarayana, V. S. S. Sastry, H. Takezoe, N. V. Madhusudana and S. Dhara, *Phys. Rev. E: Stat., Nonlinear, Soft Matter Phys.*, 2010, **81**, 011701.